Modeling, analysis, and design of stationary reference frame droop controlled parallel three-phase voltage source inverters

Vasquez, Juan Carlos; Guerrero, Josep M.; Savaghebi, Mehdi; Eloy-Garcia, Joaquin ; Teodorescu, Remus

Published in:
I E E E Transactions on Industrial Electronics

DOI (link to publication from Publisher):
10.1109/TIE.2012.2194951

Publication date:
2013

Document Version
Early version, also known as pre-print

Modeling, Analysis, and Design of Stationary Reference Frame Droop Controlled Parallel Three-Phase Voltage Source Inverters

Juan C. Vasquez, *Member, IEEE*, Josep M. Guerrero, *Senior Member, IEEE* Mehdi Savaghebi, *Student Member, IEEE*, Joaquin Eloy-Garcia, and Remus Teodorescu, *Fellow Member, IEEE*

***Abstract*- Power electronics based MicroGrids consist of a number of voltage source inverters (VSIs) operating in parallel. In this paper, the modeling, control design, and stability analysis of parallel connected three-phase VSIs are derived. The proposed voltage and current inner control loops and the mathematical models of the VSIs are based on the stationary reference frame. A hierarchical control scheme for the paralleled VSI system is developed comprising two levels. The primary control includes the droop method and the virtual impedance loops, in order to share active and reactive power. The secondary control restores the frequency and amplitude deviations produced by the primary control. Also, a synchronization algorithm is presented in order to connect the MicroGrid to the grid. Experimental results are provided to validate the performance and robustness of the parallel VSI system control architecture.**

Keywords: **Distributed Generation (DG), Droop method, Hierarchical control, MicroGrid (MG), Voltage Source Inverters.**

I. INTRODUCTION

RECENTLY, MicroGrids (MGs) are emerging as a framework for testing future SmartGrid issues in small scale. In addition, power electronics-based MGs are useful when integrating renewable energy resources, distributed energy storage systems and active loads. Indeed, power electronic equipment is used as interface between those devices and the MG. This way, MG can deal with power quality issues as well as increase its interactivity with the main grid or with other MGs, thus creating MG clusters [1].

Voltage source inverters (VSIs) are often used as a power electronics interface; hence, the control of parallel VSIs forming a MG has been investigated in recent years [1-9]. Decentralized and cooperative controllers such as the droop method have been proposed in the literature. Further, in order to enhance the reliability and performances of the droop controlled VSIs, virtual impedance control algorithms have been also developed, providing to the inverters with hot-swap operation, harmonic power sharing and robustness for large line power impedances variations [10]. Droop control is a kind of cooperative control that allows parallel connection of VSIs sharing active and reactive power. It can be seen as a primary power control of a synchronous machine.

However, the price to pay is that power sharing is obtained through voltage and frequency deviations of the system [11], [12]. Thus, secondary controllers are proposed in order to reduce them, like those in large electric power systems [1]. Hence, the MG can operate in island mode, restoring the frequency and amplitude in spite of deviations created by the total amount of active and reactive power demanded by the loads [11].

Island operation mode is an old concept that, for example, constitutes the basis of Uninterruptible Power Supply (UPS), which is responsible for supplying critical loads under grid faults [10], [11]. Nevertheless, UPS systems are designed with different purposes than those in MGs. Thus, MGs are not conceived to work as a closed system, but they are an easy-to-expand system capable of integrating distributed generation (DG) systems, distributed storage (DS) elements and dispersed loads.

In the case of transferring from islanded operation to grid connected mode, it is necessary to first synchronize the MG to the grid. Thus, a distributed synchronization control algorithm is necessary [1]. Once the synchronization is reached, a static transfer switch connects the MG to the grid or to a MG cluster. After the transfer process between islanded and grid-connected modes is finished, it is necessary to control the active and reactive power flows at the point of common coupling (PCC). This can be done by a tertiary controller that should take into account the state of charge (SoC) of the energy storage systems, available energy generation, and energy demand [7,13]. These aspects are out of the scope of this paper.

In order to implement such a kind of multilevel control algorithm, it is necessary to apply for communication systems in order to send information between the DG units [17]-[20]. The concept and general aspects needed for the future intelligent flexible MGs deployment have been developed in [21], with the flexibility of operating in both grid-connected and islanded mode.

J. C. Vasquez, J. M. Guerrero, and Remus Teodorescu are with the Institute of Energy Technology, Aalborg University, Aalborg East DK-9220, Denmark (e-mail: juq@et.aau.dk, joz@et.aau.dk, ret@et.aau.dk).

J. Eloy-Garcia is with the Department of Electrical Engineering, University Carlos III of Madrid, Spain (e-mail: jeloygar@ing.uc3m.es)

M. Savaghebi is with the Electrical Engineering Department and Center of Excellence for Power System Automation and Operation, Iran University of Science and Technology, Tehran 16846-13114 Iran (e-mail: savaghebi@iust.ac.ir).

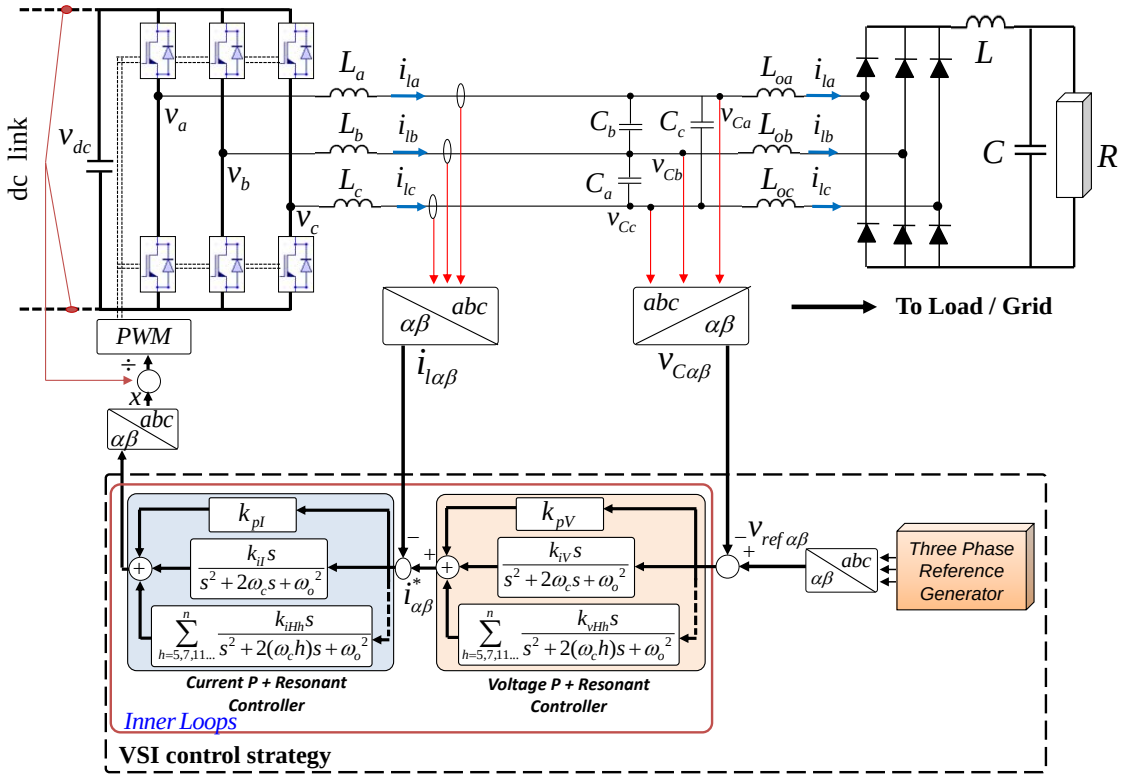

Fig.1. Block diagram of the inner control loops of a three phase VSI.

Furthermore, inner control loops design is very important for the MG performance. In [19] a resonant controller adjusted at the fundamental frequency for paralleled single-phase droop controlled inverters was proposed in order to improve the output voltage tracking feature.

In the case of three phase DG units, recently inner control loops with resonant controllers in the stationary reference frame were proposed to supply nonlinear and unbalanced local loads [17], [18].

However, droop control still has several drawbacks such as poor harmonic current sharing and high dependency on the power line impedances. In order to improve these drawbacks, some proposals were done by combining low bandwidth communications with average power sharing, droop control and extra harmonic compensation control loops [18], [19]. Also, distributed control for four-wire three-phase MGs have been proposed by using low bandwidth communications, endowing high power quality features [20].

Another possibility is to combine both master-slave and droop control techniques according to the distance of individual DG units of an islanded MG [23]. The concept is based on using master-slave control in each cluster of DG units, and droop control to balance the power between masters. It assumes that the inverters of each cluster are close enough to implement high speed communications.

Other proposals use communications between a MG central controller (MGCC) and each DG local controller. The methodology proposed by [20] and [22] is focused on using the aforementioned secondary control to restore the frequency deviation produced by the local active power/frequency droop characteristic.

In this paper, a hierarchical control for a parallel VSI system is analyzed and developed in stationary reference frame, including current and voltage control loops, virtual impedance, active/reactive power calculations and a novel $\alpha\beta$ grid synchronization algorithm. Thus in contrast to the conventional control approaches based on the synchronous reference frame, no $\alpha\beta$/dq or dq/$\alpha\beta$ transformations are required in this work. Furthermore, a secondary control and a coordinated synchronization control loop have been developed in order to restore frequency and amplitude in the MG.

The paper is organized as follows. In Section II, the system modeling and the control design of the voltage and current control loops are presented. Section III shows the droop control and virtual impedance loop designs. Section IV proposes a coordinated synchronization control loop for the MG. Section V presents the secondary control for frequency and voltage amplitude restoration. Section VI presents the experimental results of a paralleled two 2.2kW-inverter system. Finally, Section VII concludes the paper.

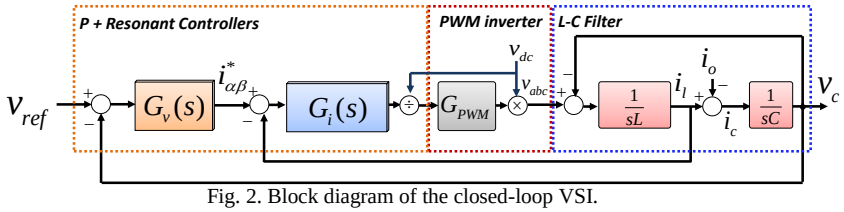

Fig. 2. Block diagram of the closed-loop VSI.

II. Inner Control Design

The control proposed for the paralleled VSI system is based on the droop control framework, which includes voltage and current control loops, the virtual impedance loop and the droop control strategy. The voltage reference v_{ref}, frequency and amplitude, will be controlled by the droop functions, generated in *abc* and transformed to $\alpha\beta$-coordinates. The $\alpha\beta$-coordinates variables are obtained by using the well-known Clarke transformation. Also, currents and voltages are transformed from *abc* to $\alpha\beta$.

Fig. 1 shows the power stage of a VSI consisting of a three phase PWM inverter and an *LCL* filter. This *LCL* filter may exhibit a critically unstable response when trying to control the output current with the inverter voltage, as can be deduced from its transfer function [4]. However, this is not the case in this paper, in which the capacitor voltage and inverter current are controlled, thus it can be seen as an *LC* filter plus an additional L_o.

The proposed controller is based on the stationary reference frame, including voltage and current control loops. These control loops include proportional + resonant (PR) terms tuned at the fundamental frequency, 5th, 7th, and 11th harmonics. Not only current control loop includes current harmonic tracking in order to supply nonlinear currents to nonlinear loads, but also voltage control loop includes that, since it is necessary to suppress voltage harmonics produced by this kind of loads. [4].

The voltage and current controllers are based on a PR structure, where generalized integrators (GI) are used to achieve zero steady-state error. Based on the *abc*/$\alpha\beta$ coordinate transformation principle, a three-phase system can be modeled in two independent single-phase systems [4]. Thus, the control diagram can be expressed and simplified as depicted in Fig 2. In order to analyze the closed-loop dynamics of the system, the Mason's theorem is applied for block diagram reduction purposes and the following transfer function is derived from Fig. 2:

$$v_c(s)=\frac{G_v(s)G_i(s)G_{PWM}}{LCs^2+\left(Cs+G_v(s)\right)G_i(s)G_{PWM}+1}v_{ref}(s)+ -\frac{Ls+G_i(s)G_{PWM}}{LCs^2+\left(Cs+G_v(s)\right)G_i(s)G_{PWM}+1}i_o(s) \quad (1)$$

being v_{ref} the voltage reference, i_o the output current, L the filter inductor value, and C the filter capacitor value. The transfer functions of the voltage controller, current controller, and PWM delay, shown in (1), are described as follows:

$$G_v(s)=k_{pV}+\frac{k_{rV}s}{s^2+{\omega_o}^2}+\sum_{h=5,7,11}\frac{k_{hV}s}{s^2+\left(\omega_o h\right)^2} \quad (2)$$

$$G_i(s)=k_{pI}+\frac{k_{rI}s}{s^2+{\omega_o}^2}+\sum_{h=5,7,11}\frac{k_{hI}s}{s^2+\left(\omega_o h\right)^2} \quad (3)$$

$$G_{PWM}(s)=\frac{1}{1+1.5T_s s} \quad (4)$$

where k_{pV} and k_{pI} are the proportional term coefficients, k_{rV} and k_{rI} are the resonant term coefficients at ω_o = 50 Hz, k_{hV} and k_{hI} are the resonant coefficient terms for the harmonics h (5th, 7th, and 11th), and T_s is the sampling time. By using the closed loop model described by equations (1)-(4), the influence of the control parameters over the fundamental frequency can be analyzed by using the Bode diagrams shown in Fig. 3. Notice that the control objective is not only to achieve a band pass filter closed loop behavior with narrow bandwidth, with 0 dB gain, but also to avoid resonances in the boundary.

Fig. 4 shows similar Bode plots regarding 5th and 7th harmonic tracking. Harmonic tracking is required for both current and voltage loops.

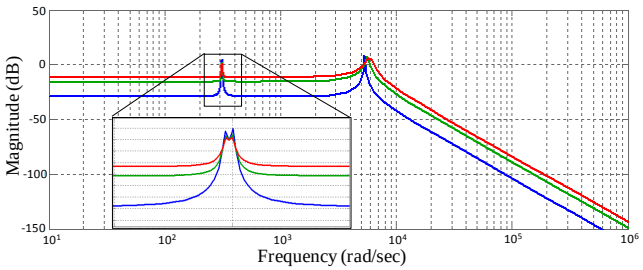

Fig.3. Bode plot of the sensitivity transfer function for different parameters of the PR controllers without harmonic compensation. k_{pV} = [0.1 1] and k_{pI} = 1.

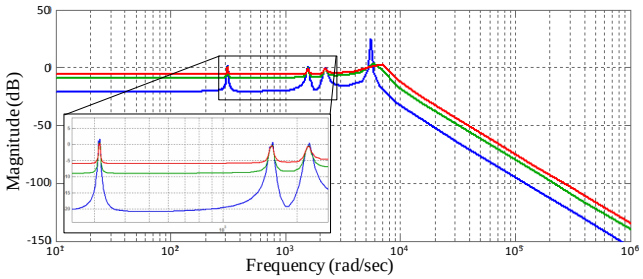

Fig.4. Bode plot of sensitivity transfer function for different PR controllers with 5th and 7th harmonic compensation. k_{pV} = [0.1 1] and k_{pI} = 1.

III. Droop Control and Virtual Impedance Loop

With the objective of paralleling VSI units, the reference of the voltage control loop v_{ref} will be generated, together with the droop controller and a virtual impedance loop. The droop control is responsible for adjusting the phase and the amplitude of the voltage reference according to the active and reactive powers (P and Q), ensuring P and Q flow control. The droop control functions can be defined as follow:

$$\phi = \phi^* - G_p(s)\left(P - P^*\right) \tag{5}$$

$$E = E^* - G_Q(s)\left(Q - Q^*\right) \tag{6}$$

being ϕ the phase of V_{ref}, ϕ^* is the phase reference $\phi^* = \omega^* \int dt = \omega^* t$, P^* and Q^* are the active and reactive power references normally set to zero, and $G_p(s)$ and $G_Q(s)$ are the compensator transfer functions, which are selected as follows:

$$G_P(s) = \frac{k_{pP}s + k_{iP}}{s} \tag{7}$$

$$G_Q(s) = k_{pQ} \tag{8}$$

being k_{iP} and k_{pQ} the static droop coefficients, while k_{pP} can be considered as a virtual inertia of the system, also known as transient droop term. The static droop coefficients k_{iP} and k_{pQ} can be selected taking into account the following relationships $k_{iP} = \Delta f/\Delta P$ (maximum frequency deviation/nominal active power) and $k_{pQ} = \Delta V/\Delta Q$ (maximum amplitude deviation/nominal reactive power).

Fig. 5 shows the block diagram of the droop control implementation. It consists of a power block calculation that calculates P and Q in the $\alpha\beta$-coordinates by using the following well-known relationship [16]:

$$p = v_{c\alpha} \cdot i_{o\alpha} + v_{c\beta} \cdot i_{o\beta} \tag{9}$$

$$q = v_{c\beta} \cdot i_{o\alpha} - v_{c\alpha} \cdot i_{o\beta} \tag{10}$$

being p and q the instantaneous active and reactive power, $v_{c\alpha\beta}$ and $i_{o\alpha\beta}$ the capacitor voltage and the output current. In order to eliminate p and q ripples, low pass filters are applied to obtain P and Q.

Furthermore, a virtual impedance loop has also been added to the voltage reference in order to fix the output impedance of the VSI which will determine the P/Q power angle/amplitude relationships based on the droop method control law.

Fig.5 depicts the implementation of the virtual impedance loop. Although the series impedance of a generator is mainly inductive due to the LCL filter, the virtual impedance can be chosen arbitrarily. In contrast with physical impedance, this virtual output impedance has no power losses, and it is possible to implement resistance without efficiency losses. The virtual impedance loop can be expressed in $\alpha\beta$-coordinates as follows [14]:

$$\begin{cases} v_{v\alpha} = R_v \cdot i_{o\alpha} - \omega L_v \cdot i_{o\beta} \\ v_{v\beta} = R_v \cdot i_{o\beta} + \omega L_v \cdot i_{o\alpha} \end{cases} \tag{11}$$

being R_V and L_V the virtual resistance and inductance value, and $v_{v\alpha,\beta}$ and $i_{o\alpha,\beta}$ the voltage and output current in $\alpha\beta$-frame.

The closed-loop modeling and the stability analysis of the virtual impedance loop has been studied in previous works [10], [19] and will be not addressed in this paper.

IV. Coordinated Synchronization Loop

In order to synchronize all the VSI of the MG, a coordinated synchronization loop is necessary to synchronize the MG with the grid. In this section, a synchronization control loop in stationary reference frame is proposed as shown in Fig. 6.

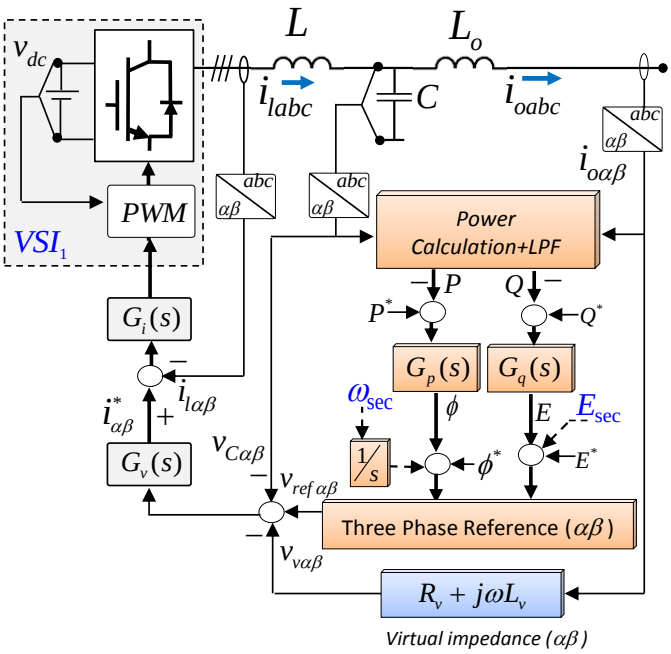

Fig.5. Block diagram of the droop controller and the virtual output impedance in $\alpha\beta$-coordinates.

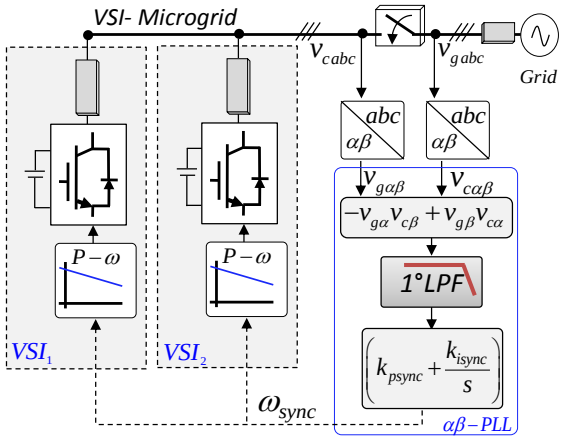

Fig.6. Block diagram of the synchronization control loop of a droop controlled MG.

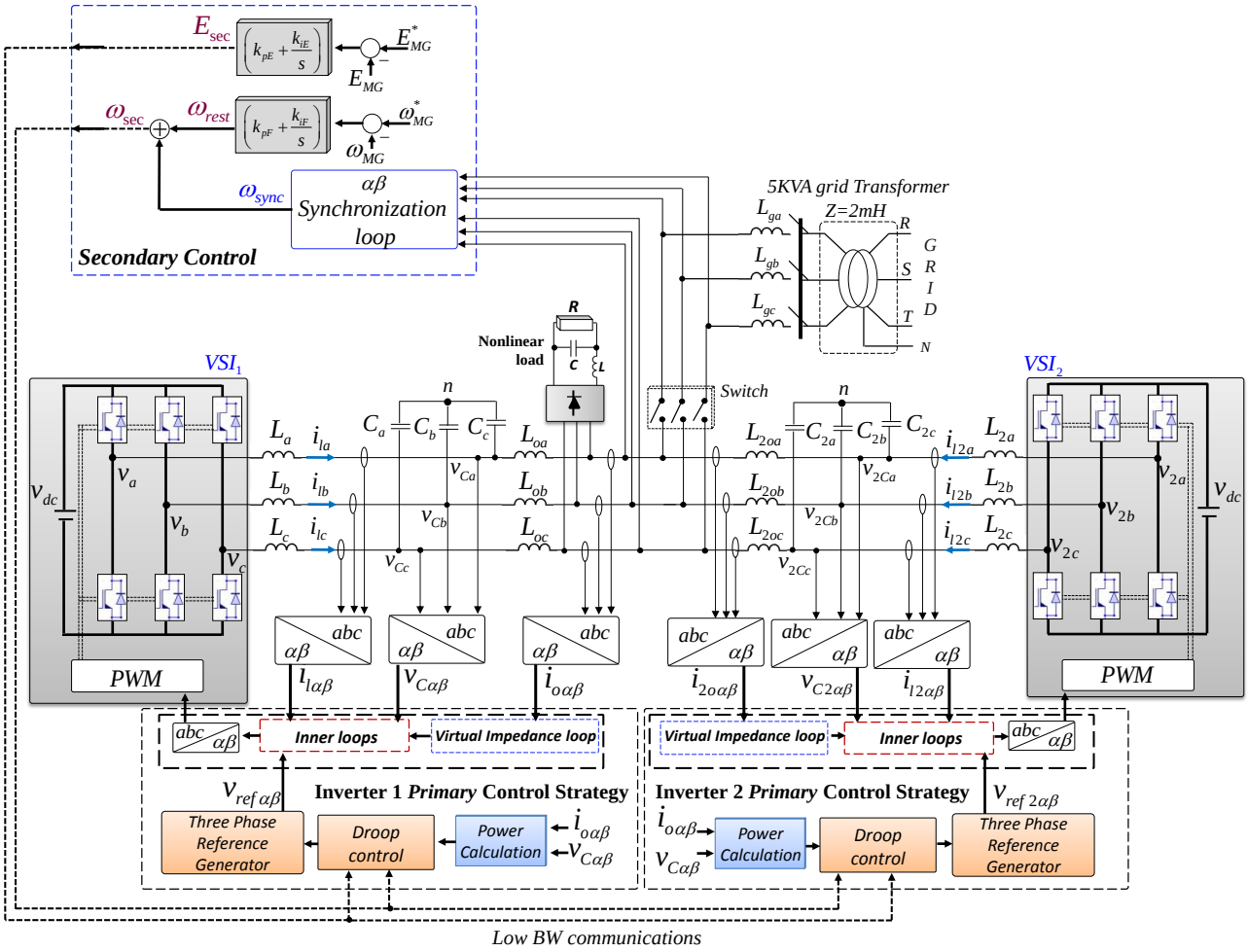

Fig. 7. Block diagram of the whole control system of two VSIs forming a MG.

The synchronization process is done by using the alpha-beta components of the grid and the VSI voltages variables, $v_{g\alpha\beta}$ and $v_{c\alpha\beta}$. Thus, when both voltages are synchronized, we can assume that

$$\left\langle v_{g\beta} v_{c\alpha} - v_{g\alpha} v_{c\beta} \right\rangle = 0 \tag{12}$$

being <x> the average value of the variable *x* over the grid frequency. Thus, we can easily derive the following PLL structure, which consist of this orthogonal product, a low-pass filter and a PI controller:

$$\omega_{sync} = \left(v_{g\beta} v_{c\alpha} - v_{g\alpha} v_{c\beta} \right) \frac{\omega_c}{s+\omega_c} \frac{k_p s + k_i}{s} \tag{13}$$

where k_p and k_i are the coefficients of the PI, and the signal ω_{sync} is the output of the coordinated-PLL to be sent toeach VSI to adjust their individual *P*-ω droop function, integrating and adding over the phase of the system, as it can be seen in Figs. 5 and 6. Notice that, the use of frequency data is suitable for low bandwidth communications, instead of using phase or time domain information, which would be needed for critical high-speed communications. This algorithm also reduces computational requirement without hampering the P/Q control loop performances.

V. Secondary Control for Frequency and Voltage Restoration

The secondary control is responsible for removing any steady-state error introduced by the droop control [15,16]. Taking into account the grid exigencies [25], the secondary control should correct the frequency deviation within allowable limit, e.g. ±0.1 Hz in Nordel (North of Europe) or ±0.3Hz in UCTE (Union for the Co-ordination of Transmission of Electricity, Continental Europe). This controller is also called Load-Frequency Control (LFC) in Europe or Automatic Gain Controller (AGC) in USA. The frequency and amplitude restoration compensators can be derived as [13]:

$$\omega_{rest} = k_{pF}\left(\omega^*_{MG} - \omega_{MG}\right) + k_{iF}\int\left(\omega^*_{MG} - \omega_{MG}\right)dt \tag{14}$$

$$E_{rest} = k_{pE}\left(E^*_{MG} - E_{MG}\right) + k_{iE}\int\left(E^*_{MG} - E_{MG}\right)dt \tag{15}$$

being k_{pF}, k_{iF}, k_{pE}, and k_{iE} the control parameters of the secondary control compensator. In this case, ω_{rest} and E_{rest} must be limited in order to not exceed the maximum allowed frequency and amplitude deviations. Fig. 7 shows the overall control system, considering current and voltage control loops, virtual output impedances, droop controllers, and secondary control of a MG.

A. Frequency Restoration

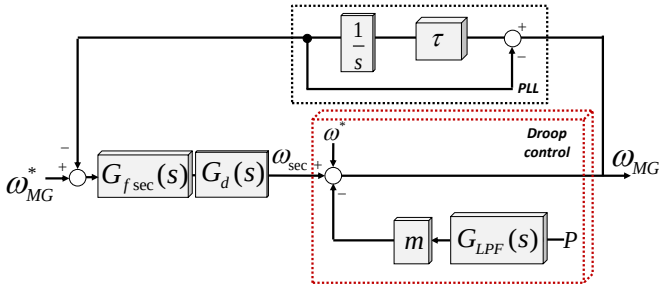

Fig.8. Block diagram of the frequency secondary control.

In order to analyze the system stability and to adjust the parameters of the frequency secondary control, a model has been developed, as can be seen in Fig. 8. The control block diagram includes the droop control of the system ($m=k_{iP}$), the simplified PLL first-order transfer function used to extract the frequency of the MG, and the secondary control $G_{fsec}(s)$, followed by a delay $G_d(s)$ produced by the communication lines. From the block diagram we can obtain the following model:

$$\omega_{MG} = \frac{G_{f\,sec}(s)G_d(s)}{1+G_{f\,sec}(s)G_d(s)G_{PLL}(s)}\omega^*_{MG} - \frac{mG_{LPF}(s)}{1+G_{f\,sec}(s)G_d(s)G_{PLL}(s)}P \tag{16}$$

where the transfer functions can be expressed as follows:

$$G_{f\,sec}(s) = \frac{k_{pF}s + k_{iF}}{s}, \tag{17}$$

$$G_{PLL}(s) = 1/(\tau s + 1), \tag{18}$$

$$G_d(s) = \frac{1}{s+1.5\omega_s}, \tag{19}$$

$$G_{LPF}(s) = \frac{\omega_c}{s+\omega_c}, \tag{20}$$

Thus, the closed loop transfer function P-to-ω_{MG} can be expressed as following:

$$\omega_{MG} = -\frac{m\omega_c s\left(s^2 + sa + b\right)}{s^4 + s^3 c + s^2 d + se + f}P \tag{21}$$

with the following parameters:

$$a = \tau + 1.5T_s$$
$$b = 1.5T_s\tau$$
$$c = 1.5T_s + \omega_c + \tau$$
$$d = \omega_c(1.5T_s + \tau) + \tau(1.5T_s + k_{pF})$$
$$e = \tau(\omega_c(k_{pF} + 1.5T_s) + k_{iF})$$
$$f = \tau k_{iF}\omega_c$$

Fig. 9 depicts the step response of the model in (21) for a P step change. This model allows us to adjust properly the control parameters of the secondary control and to study the limitations of the communications delay.

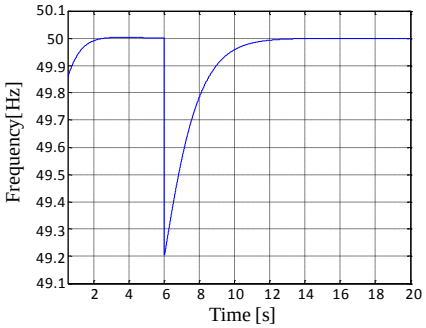

Fig. 9. Transient response of the secondary control model. for frequency restoration.

B. Amplitude Restoration

Similar procedure has been applied when designing the voltage secondary controller. Fig. 10 shows the block diagram obtained in this case.

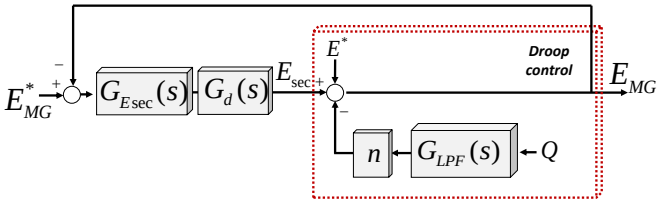

Fig.10. Block diagram of the amplitude secondary control.

Similarly, we can obtain the closed loop voltage dynamic model:

$$E^*_{MG} = \frac{G_{E\,sec}(s)G_d(s)}{1+G_{E\,sec}(s)G_d(s)}E_{sec} - \frac{nG_{LPF}(s)}{1+G_{E\,sec}(s)G_d(s)}Q \tag{22}$$

where the transfer function $G_{Esec}(s)$ is defined as follows

$$G_{E\,sec}(s) = \frac{k_{pE}s + k_{iE}}{s}. \tag{23}$$

Consequently, the following transfer function Q-to-E_{MG} can be obtained:

$$E_{MG} = -\frac{n\omega_c s(s+1.5)}{s^3 + as^2 + bs + k_{iE}\omega_c}Q \tag{24}$$

being:

$$a = k_{pE} + \omega_c + 1.5$$
$$b = \omega_c(k_{pE} + 1.5) + k_{iE}$$
$$c = k_{iE}\omega_c$$

By using this model, the dynamics of the system for a step change in Q can be obtained as shown in Fig. 11.

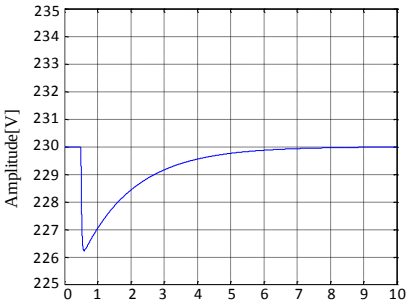

Fig. 11. Transient response of the secondary control model for amplitude restoration

VI. EXPERIMENTAL RESULTS

In order to test the feasibility of the theoretical analysis done, an experimental MG setup was built as depicted in Fig. 12 with the parameters described in Table I. Fig. 13 shows the electrical scheme and the experimental setup consisting of two Danfoss 2.2kW inverters, voltage and current LEM sensors, *LCL* filters, and a dSPACE1103 to implement the proposed control algorithms.

TABLE I
CONTROL SYSTEM PARAMETERS

Parameter	Symbol	Value	Units
Power stage			
Grid Voltage	V_g	311	V
Grid Frequency	f	50	Hz
Output Inductance	L_o	1.8	mH
Filter inductance	L	1.8	mH
Filter Capacitance	C	25	µF
Load	R_L	200/400	Ω
dc Voltage	V_{dc}	650	V
Voltage/Current P+R Control			
Voltage Loop PR	k_{pV}, $k_{rV,}$ $k_{vH5,7,11}$	0.35, 400, 4, 20, 11	
Current Loop PR	k_{pI}, $k_{rI,}$ $k_{IH5,7,11}$	0.7, 100, 30,30,30	
Primary Control			
Integral frequency droop	k_{iP}	0.0015	W/rd
Proportional frequency droop	k_{pP}	0.0003	Ws/rd
Proportional amplitude droop	k_{pQ}	0.27	VAr/V
Virtual Resistance	R_v	1	Ω
Virtual Inductance	L_v	4	mH
Secondary Control			
Frequency Proportional term	k_{pF}	0.0005	-
Frequency Integral term	k_{iF}	0.1	s^{-1}
Amplitude Proportional term	k_{pE}	0.0001	-
Amplitude Integral term	k_{iE}	0.11	s^{-1}
PLL gain	τ	50	ms

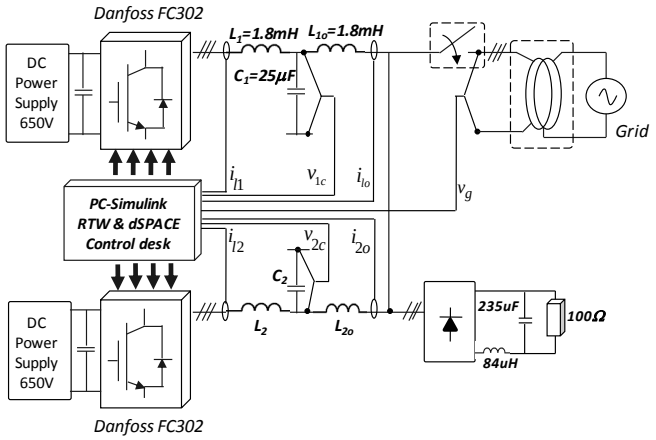

Fig. 12. Scheme of the experimental setup

The switching frequency of the inverters was set at 10 kHz. The MG was connected to the grid through a 10kVA transformer with 2mH leakage equivalent inductance. Fig. 12 also shows a nonlinear load consisting of a three-phase rectifier loaded by an LC filter and a resistor. The first test starts with the harmonic control loop disabled (Voltage THD=5.61%); and then, the voltage P+R harmonic control (Voltage THD=0.63%) is activated. Figs. 14a and 14b show the inverter output voltage and current waveforms of a standalone VSI when supplying the nonlinear load. Fig. 15 shows the output current waveforms of the two parallel connected VSIs sharing the nonlinear load by using the droop method. First, both inverters are sharing the load, and then at t=0.21s the first inverter is suddenly disconnected, letting only one VSI supplying the total amount of the needed current. Thus, if one inverter trips and the second one is able to supply the load, the system will still remain stable. This fact highlights the reliability of the system.

Fig. 16 shows how the VSIs frequency and amplitude restoration can be achieved by means of the secondary control strategy. Notice that frequency and rms voltage values are slowly and successfully regulated inside the islanded MG, removing the static deviations produced by the droop method and the virtual impedance control loops. In Fig. 16a and Fig. 16b, frequency and amplitude deviations produced by the droop method are shown at t=1.2s when a load is suddenly connected to the system. At t=8.5s, the restoration process by the secondary control of both parameters starts to act.

Fig. 17 depicts the transient response of the MG when the secondary control is continuously operating, and a load change is suddenly produced at t=9s and the second inverter is disconnected at t=31s. Note that the frequency is restored in both cases. As the MicroGrid is a small system based on power electronics, the response is faster than those shown in [25] demanded by the grid. Notice the smooth recovery towards the nominal frequency and amplitude.

Finally, Fig. 18 shows the synchronization process between the DG unit and the grid. It can be seen that the voltage waveforms of the MG and the grid are synchronizing, and the error difference between them is decreasing. This result depicts the seamless distributed synchronization process. The cooperative synchronization algorithm does not

affect the system stability since the bandwidth is much more reduced.

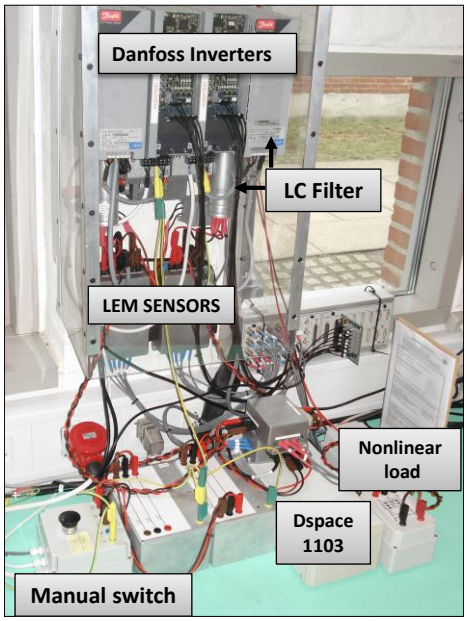

Fig. 13. Experimental setup.

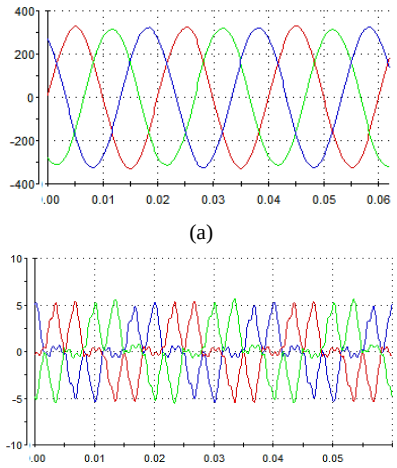

(a)

(b)

Fig. 14. Output voltage (a) and current (b) waveforms of a VSI.

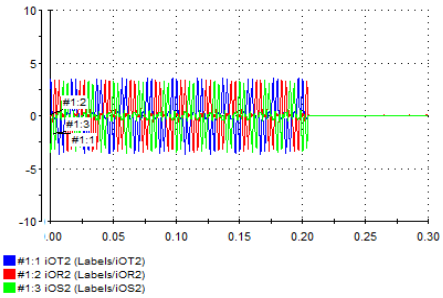

(a)

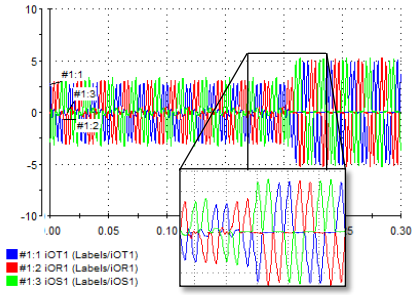

(b)

Fig. 15. Transient response of the output currents (a) inverter #1 (b) inverter #2, when inverter #1 is suddenly disconnected.

VII. CONCLUSIONS

In this paper, a hierarchical control for three-phase paralleled VSI based MGs has been proposed. The control structure was based on the stationary reference frame, and organized in two control levels. The inner control loops of the VSIs consisted of the current and voltage loops with harmonic resonant controllers. The primary control is based on the droop control and the virtual impedance concepts. The secondary control is the local centralized controller responsible for power sharing and it has the objective of restoring the frequency and amplitude deviations produced by the primary control.

The different levels of control have been modeled and the closed-loop system dynamics has been analyzed, in order to give some guidelines for the appropriate selection of the system parameters. Simulation and experimental results have shown the good performance of the MG control system.

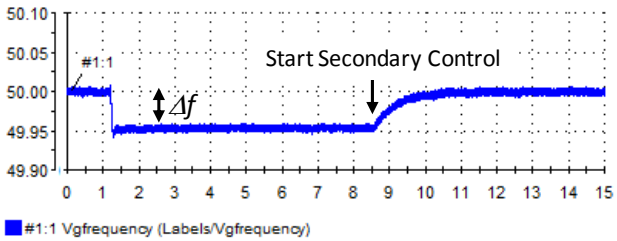

a)

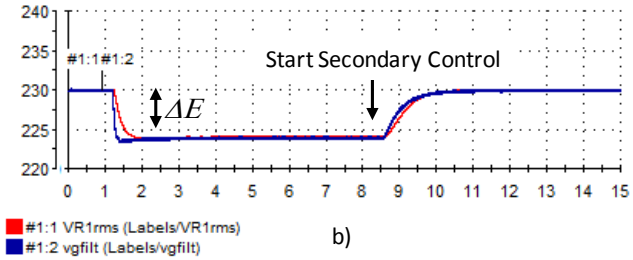

b)

Fig. 16. Frequency and amplitude deviation and restoration of the MG.

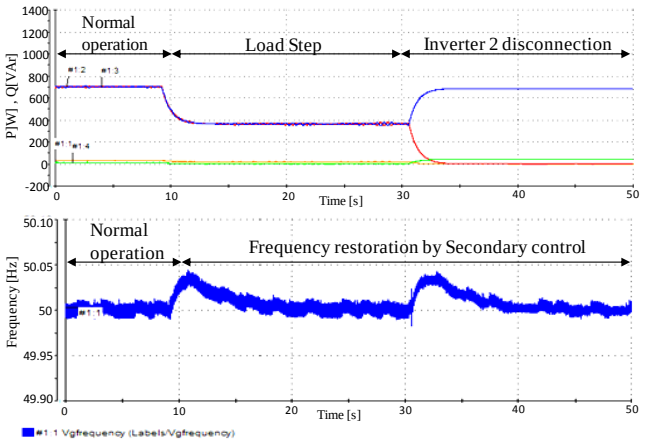

Fig. 17. Active and reactive power (top) and frequency (bottom) during load step changes (t=9s) and sudden disconnection of inverter 2 (t=31s).

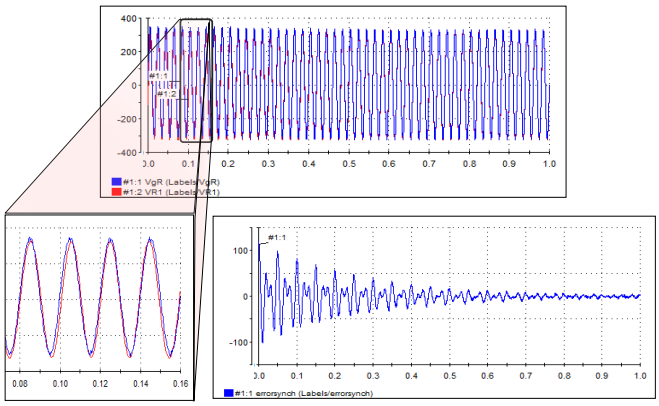

Fig. 18. Synchronization process. Top: Grid and MG Voltages, left: synchronization detail, Right: Synchronization error.

REFERENCES

[1] J. C. Vasquez, J. M. Guerrero, J. Miret, M. Castilla and L. G. de Vicuña, "Hierarchical control of intelligent microgrids," *IEEE Ind. Electron. Mag.*, vol. 4, no. 4, pp. 23 – 29, Dec. 2010.

[2] T. C. Green and M. Prodanovic, "Control of inverter-based micro-grids," *Elec. Power Sys. Research*, vol.77, no. 9, pp. 1204-1213, Jul. 2007.

[3] N. Pogaku, M. Prodanovic and T. C. Green, "Modeling, analysis and testing of autonomous operation of an inverter-based microgrid," *IEEE Trans. Power Electron.*, vol. 22, no. 2, pp.613-625, Mar. 2007.

[4] R. Teodorescu, F. Blaabjerg, M. Liserre and P. C. Loh, "Proportional-resonant controllers and filters for grid-connected voltage source converters," *IEE Proc. Electric Power Appl.*, vol.153, no.5, pp.750-762, Sept. 2006.

[5] M. B. Delghavi and A. Yazdani, "An adaptive feedforward compensation for stability enhancement in droop-controlled inverter-based microgrids," *IEEE Trans. Power Deliv.*, vol. 26, no. 3, Jul. 2011.

[6] C. K. Sao and P. W. Lehn, "Control and power management of converter fed microgrids," *IEEE Trans. Pow. Sys.*, vol. 23, no.3, pp. 1088-1098, Aug. 2008.

[7] E. Barklund, N. Pogaku, M. Prodanovic, C. Hernandez-Aramburo and T. C. Green, "Energy management in autonomous microgrid using stability-constrained droop control of inverters," *IEEE Trans. Power Electron.*, vol. 23, no.5, pp. 2346 – 2352, Sept. 2008.

[8] R. Majumder, A. Ghosh, G. Ledwich and F. Zare, "Angle droop versus frequency droop in a voltage source converter based autonomous microgrid," in *Proc. 2009 Power & Energy Soc. Gen. Meet. (PES)*, pp. 1 – 8

[9] F. Katiraei and M. R. Iravani, "Power management strategies for a microgrid with multiple distributed generation units," *IEEE Trans. Power Sys.*, vol. 21, no.4, pp. 1821 – 1831, Nov. 2006.

[10] J. M. Guerrero, J. C. Vasquez, J. Matas, M. Castilla and L. G. de Vicuna "Control strategy for flexible microgrid based on parallel line-interactive UPS systems," *IEEE Trans. Ind. Electron.*, vol. 56, no. 3, pp. 726-736, Mar. 2009.

[11] P. L. Villeneuve, "Concerns generated by islanding," *IEEE Power and Energy Mag.*, vol. 2, no. 3, pp. 49–53, May/Jun. 2004.

[12] M. C. Chandorkar, D. M. Divan and R. Adapa, "Control of parallel connected inverters in standalone ac supply systems," *IEEE Trans. Ind. Appl.*, vol. 29, no. 1, pp. 136-143, Jan./Feb. 1993.

[13] J. M. Guerrero, J. C. Vasquez, J. Matas, L. Garcia de Vicuna and M. Castilla, "Hierarchical control of droop-controlled AC and DC microgrids – a general approach towards standardization," *IEEE Trans. Ind. Electron.*, vol. 51, no. 8, pp. 158 – 172, Jan. 2011.

[14] J. He and Y. Lee, "Analysis and design of interfacing inverter output virtual impedance in a low voltage microgrid," in *Proc. 2002, IEEE ECCE Conf.*, pp.2857 – 2864.

[15] H. Matthias and S. Helmut, "Control of a three phase inverter feeding an unbalanced load and operating in parallel with other power sources," in *Proc. 2002, EPE-PEMC Conf.*, pp. 1–10.

[16] E. Hoff and T. Skjellnes, "Paralleled three-phase inverters," in *Proc. 2004, NORPIE'2004 Conf.*, pp. 1 – 6.

[17] A. Hasanzadeh, O. C. Onar, H. Mokhtari and A. Khaligh, "A proportional-resonant controller-based wireless control strategy with a reduced number of sensors for parallel-operated UPSs," *IEEE Trans. Power Deliv.*, vol. 25, no.1, pp.468-478, Jan. 2010.

[18] M. N. Marwali and A. Keyhani, "Control of distributed generation systems-part I: voltages and currents control," *IEEE Trans. Power Electron.*, vol. 19, no.6, pp. 1541- 1550, Nov. 2004.

[19] M. N. Marwali, J. Jin-Woo and A. Keyhani, "Control of distributed generation systems - part II: load sharing control," *IEEE Trans. Power Electron.*, vol.19, no.6, pp. 1551- 1561, Nov. 2004.

[20] J. A. P. Lopes, C. L. Moreira and A. G. Madureira, "Defining control strategies for microgrids islanded operation," *IEEE Trans. Power Sys.*, vol. 21, no. 2, pp. 916–924, May 2006.

[21] B. B. Kroposki, R. Lasseter, T. Ise, S. Morozumi, S. Papatlianassiou and N. Hatziargyriou, "Making microgrids work", *IEEE Power and Energy Mag.* , pp. 40–53, May/Jun. 2008.

[22] A. Mehrizi-Sani and R. Iravani, "Potential-function based control of a microgrid in islanded and grid-connected modes," *IEEE Trans. Power Sys.*, vol.25, no.4, pp.1883-1891, Nov. 2010.

[23] M. Popov, H. Karimi, H. Nikkhajoei and V. Terzija, "Modeling, control and islanding detection of microgrids with passive loads," in *Proc. 2010, Power Electron. and Motion Cont. Conf. (EPE/PEMC)*, pp.T11-107-T11-112.

[24] M. B. Delghavi and A. Yazdani, "Islanded-mode control of electronically coupled distributed-resource units under unbalanced and nonlinear load conditions," *IEEE Trans. Power Deliv.*, vol.26, no.2, pp.661-673, Apr. 2011.

[25] "Technical paper – Definition of a set of requirements to generating units," UCTE 2008.

Juan C. Vasquez received the B.S. degree in Electronics Engineering from Autonoma University of Manizales, Colombia, in 2004 where he has been teaching courses on digital circuits, servo systems and flexible manufacturing systems. In 2009, he has received his Ph.D. degree from the Technical University of Catalonia, Barcelona, Spain in 2009 at the Department of Automatic Control Systems and Computer Engineering, from Technical University of Catalonia, Barcelona Spain, where he worked as a Post-doc Assistant and also taught courses based on renewable energy systems. Currently, he is an Assistant Professor in Aalborg University, Denmark.

His research interests include modeling, simulation, and power management applied to the Distributed Generation in Microgrids.

Josep M. Guerrero (S'01–M'03–SM'08) was born in Barcelona, Spain, in 1973. He received the B.S. degree in telecommunications engineering, the M.S. degree in electronics engineering, and the Ph.D. degree in power electronics from the Technical University of Catalonia, Barcelona, Spain, in 1997, 2000 and 2003, respectively. He is an Associate Professor with the Department of Automatic Control Systems and Computer Engineering, Technical University of Catalonia, Barcelona, where he currently teaches courses on digital signal processing, FPGAs, microprocessors, and renewable energy. Since 2004, he

has been responsible for the Renewable Energy Laboratory, Escola Industrial de Barcelona. He has been a visiting Professor at Zhejiang University, China, and University of Cergy-Pontoise, France. From 2011, he is a Full Professor at the Department of Energy Technology, Aalborg University, Denmark, where he is the responsible of the Microgrids research program. His research interests is oriented to different Microgrids aspects, including power electronics, distributed energy storage systems, hierarchical and cooperative control, energy management systems and optimization of microgrids and islanded minigrids.

Dr. Guerrero is an Associate Editor for the IEEE Transactions on Power Electronics, IEEE Transactions on Industrial Electronics, and IEEE Industrial Electronics Magazine. He has been Guest Editor of the IEEE Transactions on Power Electronics Special Issues: Power Electrics for Wind Energy Conversion and Power Electronics for Microgrids; and the IEEE Transactions on Industrial Electronics Special Sections: Uninterruptible Power Supplies (UPS) systems, Renewable Energy Systems, Distributed Generation and Microgrids, and Industrial Applications and Implementation Issues of the Kalman Filter. He currently chairs the Renewable Energy Systems Technical Committee of IEEE IES.

Mehdi Savaghebi (S'06) was born in Karaj, Iran, in 1983. He received the B.S. degree from Tehran University, Iran, in 2004 and the M.S. degree with highest honors from Iran University of Science and Technology (IUST), in 2006, both in electrical engineering. He is now perusing the Ph.D. degree in IUST.

His main research interests include Distributed Generation systems, Microgrids and power quality issues of electrical systems.

Joaquin Eloy-Garcia was born in Malaga, Spain. He received the M.Sc. degree in automation and electronics engineering from the University of Malaga, Malaga, Spain, in 2002, and the Ph.D. degree in electrical engineering from the University Carlos III of Madrid, Madrid, Spain, in 2007. Since 2005, he has been an Assistant Professor with the Department of electrical Engineering, University Carlos III of Madrid. His research interests include control of electric drives and power electronics applied to renewable energies, mainly focused on wind and photovoltaic applications

Remus Teodorescu (S'96–A'97–M'99–SM'02-FM'12) received the Dipl. Ing. degree in electrical engineering from the Polytechnical University of Bucharest, Bucharest, Romania, in 1989, and the Ph.D. degree in power electronics from the University of Galati, Galati, Romania, in 1994.

From 1989 to 1990, he was with Iron and Steel Plant Galati. He then moved to the Department of Electrical Engineering, University of Galati, where he was an Assistant and has been an Assistant Professor since 1994. In 1996, he was appointed Head of the Power Electronics Research Group, University of Galati. In 1998, he joined the Power Electronics and Drives Department, Institute of Energy Technology, Aalborg University, Aalborg, Denmark, where he is currently a Full Professor. He is the coordinator of Vestas Power Program, a research project between Vestas Wind Systems A/S and Aalborg University in power electronics, power systems and energy storage areas. He has published more than 180 technical papers, two books, and five patents.

Dr. Teodorescu is an Associate Editor for the IEEE TRANSACTIONS ON POWER ELECTRONICS LETTERS and the Chair of the IEEE Danish Industry Applications Society (IAS)/Industrial Electronics Society (IES)/Power Electronics Society (PELS) chapter. He is the corecipient of the Technical Committee Prize Paper Award from the IEEE IAS Annual Meeting 1998 and the Third-ABB Prize Paper Award from IEEE Optim 2002.